

## Use of surface Brillouin scattering to examine a structural phase transition in carbon-ion-bombarded silicon during high-temperature annealing

X. Zhang, J. D. Comins,\* and A. G. Every

*School of Physics and Materials Physics Institute, University of the Witwatersrand, Johannesburg, Wits 2050, South Africa*

T. E. Derry

*School of Physics and Schonland Research Institute for Nuclear Sciences, University of the Witwatersrand, Johannesburg, Wits 2050, South Africa*

(Received 11 May 2001; published 4 December 2001)

Surface Brillouin scattering (SBS) has been used to monitor a structural transition during high-temperature annealing of silicon previously bombarded at ambient temperature with 100 keV carbon ions with a fluence of  $5 \times 10^{17}$  ions/cm<sup>2</sup>. It was observed that a significant change of the Rayleigh surface wave peak frequency occurred during annealing at 600 °C; thereafter the frequency remained essentially constant to 900 °C. Raman and SBS measurements of the sample after annealing and recooling to ambient temperature show that the significant change in the Rayleigh mode frequency results from recrystallization of the amorphous silicon layer near the sample surface produced by the ion bombardment. The work demonstrates the potential of SBS to study *in situ* the structural phase transitions of opaque materials.

DOI: 10.1103/PhysRevB.65.012106

PACS number(s): 68.35.Rh, 78.35.+c, 68.60.Bs, 61.80.Jh

It is well established that amorphous layers can be produced near the surfaces of crystalline semiconductors by high-fluence ion bombardment.<sup>1</sup> For such amorphous silicon films, epitaxial recrystallization can be achieved by high-temperature annealing, but the type and degree of residual disorder in the recrystallized layer depends on the implanted species.<sup>2</sup>

Because of their device applications, SiC buried layers in silicon created by high-fluence carbon-ion bombardment have received considerable attention.<sup>3–6</sup> As part of the SiC formation process, annealing of the samples at high temperatures subsequent to bombardment is carried out, resulting in the recrystallization of the amorphized silicon surface layer and the development of complex layer structures containing SiC crystallites in the carbon-rich regions. In these previous studies, measurements were made after the high-temperature annealing. Thus the precise temperatures at which these complex processes take place, including the recrystallization of the amorphous silicon, are not well defined; such knowledge is important for a thorough understanding of the mechanisms involved.

Surface Brillouin scattering (SBS) is the inelastic scattering of light by thermally induced surface acoustic waves (SAW's) in the gigahertz frequency range<sup>7–10</sup> and provides an effective method to characterize the elastic properties of thin supported layers. Of relevance to the present study are the reductions in the Rayleigh SAW velocity observed on silicon bombarded with 1.8 MeV Kr ions and attributed to amorphization of the structure.<sup>11</sup> Recently, SBS has been extended to high-temperature measurements of the elastic properties of silicon<sup>12</sup> and a nickel-based superalloy,<sup>13</sup> and has been used to study the melting transition of tin nanoparticles by observing the change in the frequency of the Rayleigh SAW above and below the melting temperature.<sup>14</sup> The present work uses SBS to investigate the high-temperature recrystallization of amorphous silicon formed in the carbon-ion bombardment of silicon, by means of the behavior of the Rayleigh SAW, which is monitored throughout this high-temperature transition.

Samples of dimensions  $4 \times 4$  mm<sup>2</sup> were cut from an *n*-type silicon wafer with a phosphorus dopant concentration of  $10^{16}$  cm<sup>-3</sup>, and prepared with a chemically polished (001) surface. A 3.8 mm diameter region of one sample was bombarded at ambient temperature by carbon ions of energy 100 keV to a fluence of  $5 \times 10^{17}$  ions/cm<sup>2</sup>. The ion beam was tilted about 7° away from the [001] direction to reduce ion channeling.

Using a transport of ions in matter (TRIM) 92 simulation,<sup>15</sup> the distribution of the implanted carbon ions within the sample was estimated to be as shown in Fig. 1. The carbon ions are mainly found in the region of 2000–4000 Å from the surface and to have an approximately Gaussian distribution. The calculation neglects the possible effects of carbon diffusion.<sup>4</sup> Figure 1 also shows a standard TRIM simulation of the vacancy distribution for silicon bombarded with the carbon ions. For high-fluence ion bombardments such as the present case this calculated distribution is unphysical since it neglects sequential displacements of the silicon atoms, resulting in amorphization. For the

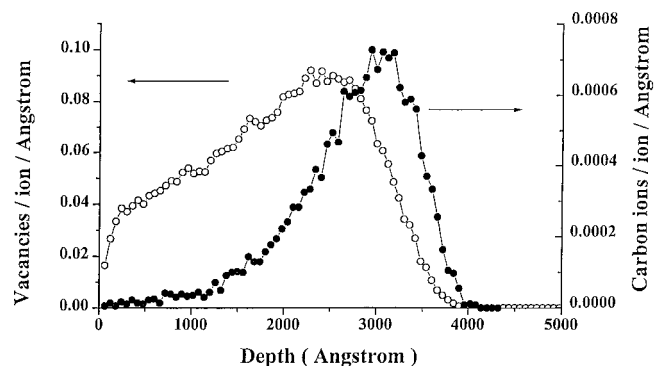


FIG. 1. The distribution of the implanted carbon ions and vacancies in the silicon calculated using a TRIM 92 simulation. The carbon ions are mainly distributed in the region of 2000 to 4000 Å and the distribution curve is approximately Gaussian in shape.

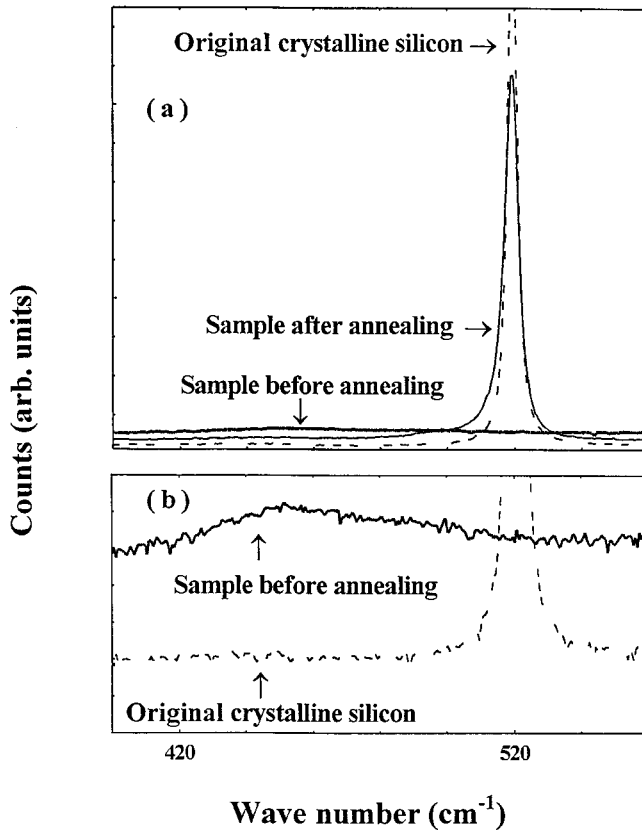


FIG. 2. Raman spectra for the original crystalline silicon and the carbon-ion-bombarded sample. (a) The crystalline silicon peak near  $520\text{ cm}^{-1}$  is completely suppressed for the carbon-ion-bombarded sample before annealing, and reappears for the sample after annealing, but with lower intensity and a larger peak width. (b) Spectra for original crystalline and carbon-ion-bombarded silicon shown on an expanded scale. The sample before annealing shows a broad peak at  $450\text{ cm}^{-1}$ , characteristic of amorphous silicon (Ref. 10).

carbon-ion fluence of  $5 \times 10^{17}$  ions/cm<sup>2</sup>, the values of the vacancy concentration within  $3600\text{ \AA}$  from the surface are more than  $0.01/\text{ion}/\text{\AA}$  yielding a vacancy concentration of greater than  $5 \times 10^{23}\text{ cm}^{-3}$  or 10 times the atomic density of silicon. In other words each silicon atom within this range has been displaced, on average, 10 times leading to this region being uniformly amorphous. The fully amorphized silicon state will not be achieved in the tail region of  $3600\text{--}4000\text{ \AA}$  from the surface, but this is only a small fraction of the amorphous layer thickness.

The original and carbon-ion-bombarded silicon samples were initially examined by Raman spectroscopy. In Fig. 2(a) it is seen that the strong crystalline silicon peak near  $520\text{ cm}^{-1}$  is completely suppressed for the carbon-ion-bombarded sample. Instead there is a weak, broad peak around  $450\text{ cm}^{-1}$  shown in detail in Fig. 2(b). This feature was reported in Refs. 11 and 16 for amorphous silicon produced by krypton- and argon-ion bombardment, respectively. Thus the present Raman studies confirm that the near surface layer is completely amorphized.

The carbon-ion-bombarded sample was also studied using SBS prior to annealing. Accounts of the experimental technique and the surface Green's-function method of analysis

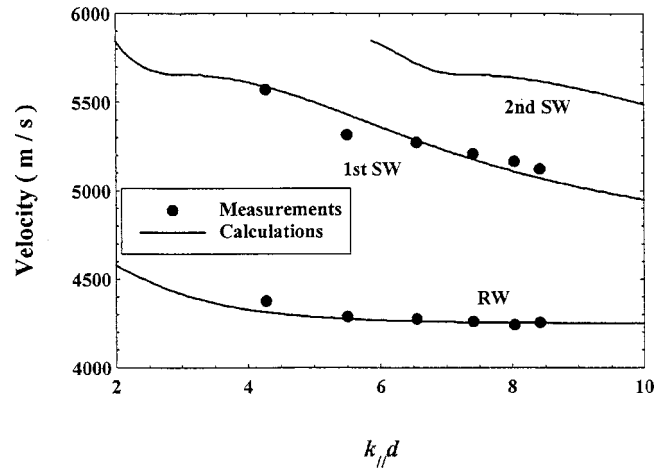


FIG. 3. The measured and calculated velocity dispersion curves of SAW modes for the carbon-ion-bombarded sample for a wave vector along the  $[100]$  direction in the  $(001)$  surface referred to the crystalline silicon substrate. The measurements are in agreement with the calculations for both the Rayleigh (RW) and the first-order Sezawa SAW (SW).

used are given in Refs. 10 and 16. A collection lens of focal length  $50\text{ mm}$  was used with slits limiting the collection aperture to minimize errors due to aperture effects.<sup>17</sup> Figure 3 shows the measured velocity dispersion relations of the Rayleigh and first-order Sezawa SAW's for the carbon-ion-bombarded sample for a wave vector along the  $[100]$  direction in the  $(001)$  surface referred to the crystalline silicon substrate. In this diagram,  $k_{\parallel}d$  is the product of the SAW wave vector and layer thickness. The Rayleigh SAW velocity levels off at a value of  $4250\text{ m/s}$  for  $k_{\parallel}d$  larger than about 6, consistent with our previous measurements on ion-beam amorphized silicon.<sup>16</sup>

In the calculation of the velocity dispersion relations, the system is modeled simply as a single amorphous silicon layer of thickness  $3600\text{ \AA}$  on a crystalline silicon substrate; this effectively neglects the effects of the implanted carbon ions. For the calculation, the material constants of both the substrate and the ion-bombarded layer are required. For crystalline silicon we use the values from Ref. 18, namely, mass density  $\rho = 2.332\text{ g/cm}^3$  and  $C_{11} = 165.7$ ,  $C_{12} = 63.9$ , and  $C_{44} = 79.6\text{ GPa}$ . The density of amorphous silicon produced by ion bombardment has been measured by Custer *et al.*<sup>19</sup> as  $2.290\text{ g/cm}^3$  (rather than the value of  $2.215\text{ g/cm}^3$  for sputtered amorphous silicon used in determining the elastic constants for the ion-amorphized silicon layer in Ref. 16). Using this revised value for the density of the amorphous silicon layer, we have recalculated the elastic constants of amorphous silicon using the experimental data of Ref. 16; the results are  $C_{11} = 143$  and  $C_{44} = 49.6\text{ GPa}$ . Using these values, the velocity dispersion curves for the carbon-ion-bombarded sample were calculated and are shown in Fig. 3. It is seen that the measured dispersion curves for the Rayleigh and the first Sezawa modes are in a good agreement with the calculation. It is apparent that the form of the carbon ions within the amorphous silicon prior to annealing does not significantly alter its elastic properties, as assumed implicitly in the simple model adopted.

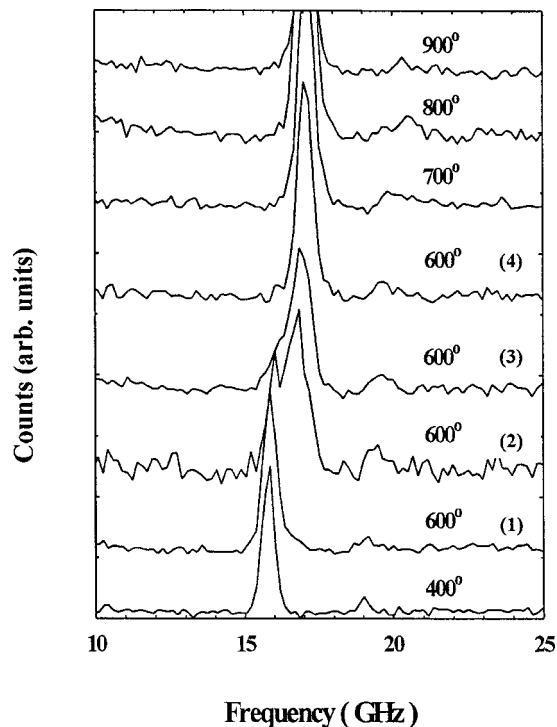


FIG. 4. The anti-Stokes SBS spectra for the carbon-ion-bombarded sample taken along the [100] direction referred to the (001) silicon substrate at different temperatures. At 600 °C, a broadened peak was observed in the second measurement, indicating that a structural transition occurred. Spectra at 600 °C labeled as (1), (2), (3), and (4) signify a succession of spectra measured at time intervals of 20 min.

The carbon-ion-bombarded sample was mounted in an optical furnace adapted for SBS measurements and operated in a vacuum of  $10^{-5}$  Torr. Light of wavelength 514.5 nm from an argon-ion laser operated in a single axial mode illuminated the sample using an incident angle of  $70.7^\circ$ . The scattered light was collected by a 120 mm focal length lens of aperture  $f$  5.5 in a backscattering geometry. The sample was successively annealed in the furnace at a series of temperatures from room temperature to 900 °C. The sample was first raised to each chosen temperature within a period of about half an hour. During this period of heating the SBS spectrum was acquired, in order to detect possible changes in the Rayleigh SAW peak. When the desired annealing temperature had been reached, SBS spectra were collected to monitor the SAW behavior for the sample during annealing; each spectrum took about 20 min to acquire. This procedure was continued until the observed SAW peak ceased shifting at the set temperature. The sample was then heated to the next temperature and the procedure repeated. The annealing series was terminated after 900 °C, as the sample surface started to deteriorate.

Figure 4 shows the anti-Stokes SBS spectra for the sample taken along the [100] direction referred to the (001) crystalline silicon surface at the different annealing temperatures. The respective spectra have been measured for the same data-accumulation times and have been offset for the convenience of comparison. The last spectrum acquired at

each temperature is shown (except at 600 °C), because it provides the stable SAW peak for that set temperature. At 400 °C or below, there is no significant change of the peak shape of the Rayleigh SAW, while the phase velocity of the mode increases by about 0.8% from room temperature to 400 °C. At 600 °C, the Rayleigh SAW peak in spectrum (1) (and during the heating period) remains essentially unchanged. In spectrum (2) at 600 °C, the originally sharp Rayleigh peak broadens significantly. It still has its leading edge close to 16 GHz, the position of the Rayleigh peaks observed previously, but its trailing edge extends to about 17.5 GHz. In spectrum (3), the broadened peak becomes somewhat sharper again, with the peak position shifting about 7% to higher frequencies and with a small shoulder on the leading edge. In spectrum (4), a sharp Rayleigh peak is again observed but with its peak at 17.5 GHz. There is no significant change of the peak position in the spectra obtained after further annealing at this temperature. At 700 °C, the frequency of the Rayleigh SAW peak shifts slightly to higher frequency (by 0.6%), but there is no observable change in the shape of the peak. At 800 °C and 900 °C, there is no significant change in peak position and peak shape for the sample.

For bulk materials or thin films of sufficient thickness, the true Rayleigh SAW peak has a Lorentzian line shape with a linewidth of about 0.5 GHz. Peaks of this nature are shown in Fig. 4 for spectra measured at 400 °C and above 700 °C. It is evident that at 600 °C, the Rayleigh SAW peak of the sample undergoes a significant variation both in its line shape and peak frequency; indeed spectrum (2) displays a broad double peak indicating a change in the elastic properties near the surface. With increasing annealing time at 600 °C a new and sharp peak emerges at a higher frequency with a frequency shift of about 1.5 GHz as shown by a comparison of spectra (1) and (4). This substantial increase of the Rayleigh SAW frequency during annealing is indicative of a structural transition and the presence of an elastically stiffer phase in the near surface region.

The annealed sample was recooled to room temperature and removed for Raman measurements. The postannealing Raman spectrum is also shown in Fig. 2. It is observed that the crystalline silicon peak near  $520\text{ cm}^{-1}$  reappears for the sample after annealing but with a lower intensity and larger peak width (with the same incident laser power and spectral acquisition time). No additional Raman peak is present in the spectrum. The results indicate that the amorphous silicon layer near the sample surface had recrystallized; the lower intensity and larger peak width indicate that the recrystallized silicon is not as perfect as the original crystal.

The formation of an elastically stiff carbide phase<sup>3-6</sup> near the surface is not considered a likely explanation of the significant shifts of the Rayleigh peak during annealing at 600 °C since (i) carbide phases were previously observed only in samples annealed at temperatures above 800 °C–900 °C, (ii) the Raman spectrum after annealing does not provide evidence of a carbide phase, and (iii) for the 100 keV carbon-ion-bombarded silicon, experiments<sup>6</sup> indicate that for annealing at 900 °C and 1000 °C, the SiC formation is initiated in the region of a sufficiently large carbon-to-silicon

ratio, near the peak of the implanted carbon-ion distribution, which is located more than 2000 Å below the sample surface. Thus point (iii) indicates that a carbide layer, even if formed, would be too deep below the surface to significantly influence the Rayleigh SAW velocity. We thus conclude that the substantial shift of the Rayleigh peak in SBS spectra for the sample during 600 °C annealing in Fig. 4 is solely caused by the recrystallization of the amorphous silicon near the sample surface.

By combining the results of the Raman and SBS measurements with those of the TRIM calculations, it is possible to explain the behavior of the Rayleigh SAW observed during annealing in some detail. From room temperature to 400 °C, the layer structures in the sample apparently remain nearly the same. However during annealing, it is expected that the displaced silicon atoms, vacancies, and implanted carbon ions will be redistributed and some bombardment-induced defects will be annealed. This process results in an increase in the Rayleigh SAW velocity with increasing temperature, which is contrary to the results of high-temperature SBS measurements of crystalline silicon.<sup>12</sup> During the first stages of the 600 °C annealing, the dominant process is the annealing of defects; here the Rayleigh SAW peaks shift only slightly. Subsequently the recrystallization process starts and significantly changes the Rayleigh SAW peak. It is clear that the recrystallization rate is relatively slow; the peak shifts over the 20 min collection time, resulting in a broad feature being formed. Thus its leading edge is close to the position

of the Rayleigh peaks observed previously and it will have a trailing edge extending to higher frequencies. For the next spectrum, the recrystallizing silicon layer is still growing and has a considerable thickness, therefore the broad peak becomes sharp again with only a small shoulder on the leading edge. Continuous annealing at 600 °C results in the recrystallizing layer growing yet more slowly, resulting in the Rayleigh SAW peak being maintained at nearly the same position during the collection time. Increasing the temperature to 700 °C, the recrystallizing layer thickness increases, bringing another 0.6% shift of the Rayleigh SAW peak position. During the annealing at 800 °C and 900 °C, any effect of further recrystallized silicon on the Rayleigh SAW peak can only counteract the effects of the lowering of the peak frequency with increasing temperature, and therefore the peak remains at nearly the same position.

In conclusion, the SBS technique has been used to monitor a structural transition in carbon-ion-bombarded silicon during high-temperature annealing. The combination of SBS, Raman scattering, and TRIM simulations have provided information on the process of recrystallization of an amorphous silicon film. Brillouin scattering applied to studies of phase transitions in transparent materials is well established,<sup>20</sup> and includes studies at high temperature (see, e.g., Ref. 21). The present work demonstrates the potential of the SBS technique for *in situ* monitoring of structural phase transitions in opaque materials.

\*Corresponding author. Email address:

comins@physnet.phys.wits.ac.za

<sup>1</sup>J. M. Poate, in *Amorphous Silicon and Related Materials*, edited by H. Fritzsche (World Scientific, Singapore, 1988), Vol. A, p. 149.

<sup>2</sup>T. E. Seidel, R. L. Meek, and A. G. Cullis, *J. Appl. Phys.* **46**, 600 (1975).

<sup>3</sup>I. P. Akimchenko, K. V. Kisseleva, V. V. Krasnopevtsev, A. G. Touryansky, and V. S. Vavilov, *Radiat. Eff.* **48**, 7 (1980).

<sup>4</sup>T. Kimura, S. Kagiya, and S. Yugo, *Thin Solid Films* **94**, 191 (1982).

<sup>5</sup>K. Srikanth, M. Chu, S. Ashok, N. Nguyen, and K. Vedam, *Thin Solid Films* **163**, 323 (1988).

<sup>6</sup>K. Kh. Nussupov, N. B. Bejsenkanov, and J. Tokbakov, *Nucl. Instrum. Methods Phys. Res. B* **103**, 161 (1995).

<sup>7</sup>J. R. Sandercock, in *Light Scattering in Solids III, Topics in Applied Physics*, edited by M. Cardona and G. Guntherodt (Springer, Berlin, 1982), Vol. 51, p. 173.

<sup>8</sup>F. Nizzoli and J. R. Sandercock, in *Dynamical Properties of Solids*, edited by G. K. Horton and A. A. Maradudin (North-Holland, Amsterdam, 1990), Vol. 6, p. 281.

<sup>9</sup>P. Mutti, C. E. Bottani, G. Ghisloti, M. Beghi, G. A. D. Briggs, and J. R. Sandercock, in *Advances in Acoustic Microscopy*, edited by A. Briggs (Plenum, New York, 1995), Vol. 1, p. 249.

<sup>10</sup>J. D. Comins, in *Handbook of Elastic Properties of Solids, Liquids and Gases, Dynamic Methods for Measuring the Elastic Properties of Solids*, edited by A. G. Every and W. Sachse (Academic, New York, 2001), Vol. 1, p. 349.

<sup>11</sup>R. Bhadra, J. Pearson, P. Okamoto, L. Rehn, and M. Grimsditch, *Phys. Rev. B* **38**, 12 656 (1988).

<sup>12</sup>P. R. Stoddart, J. D. Comins, and A. G. Every, *Phys. Rev. B* **51**, 17 574 (1995); *Physica B* **219&220**, 717 (1996).

<sup>13</sup>X. Zhang, P. R. Stoddart, J. D. Comins, and A. G. Every, *J. Phys.: Condens. Matter* **13**, 2281 (2001).

<sup>14</sup>C. E. Bottani, A. Li Bassi, B. K. Tanner, A. Stella, P. Tognini, P. Cheyssac, and R. Kofman, *Phys. Rev. B* **59**, R15 601 (1999).

<sup>15</sup>J. F. Ziegler, J. P. Biersack, and U. Littmark, *The Stopping and Range of Ions in Solids* (Pergamon, New York, 1985).

<sup>16</sup>X. Zhang, J. D. Comins, A. G. Every, P. R. Stoddart, W. Pang, and T. E. Derry, *Phys. Rev. B* **58**, 13 677 (1998).

<sup>17</sup>P. R. Stoddart, J. C. Crowhurst, A. G. Every, and J. D. Comins, *J. Opt. Soc. Am. B* **15**, 2481 (1998).

<sup>18</sup>G. W. Farnell and E. L. Adler, in *Physical Acoustics*, edited by W. P. Mason and R. W. Thurston (Academic, New York, 1972), Vol. 9, p. 35; G. W. Farnell, in *Physical Acoustics*, edited by W. P. Mason and R. W. Thurston (Academic, New York, 1970), Vol. 6, p. 109.

<sup>19</sup>J. S. Custer, M. O. Thompson, D. C. Jacobson, J. M. Poate, S. Roorda, W. C. Sinke, and F. Spaepen, *Mater. Res. Soc. Symp. Proc.* **157**, 689 (1990).

<sup>20</sup>H. Z. Cummins, in *Light Scattering Near Phase Transitions*, edited by H. Z. Cummins and A. P. Levanyak (North-Holland, Amsterdam, 1983), p. 359.

<sup>21</sup>J. D. Comins, P. E. Ngoepe, and C. R. A. Catlow, *J. Chem. Soc., Faraday Trans.* **86**, 1183 (1990).